PROGRAMME OF THE EUROPEAN UNION

GALILEO EGNOS

DLR

EUROPEAN GNSS (GALILEO)
OPEN SERVICE

NTCM-G IONOSPHERIC MODEL DESCRIPTION

Terms of Use and Disclaimers

This document describes the *NTCM G* ionospheric model developed for the Galileo satellite navigation system that can be used to determine Galileo single-frequency ionospheric corrections. Its content has been prepared and scrutinized by various groups of specialized scientists. The model has been characterized and thoroughly tested and provides excellent performance similar to the current recommended solution using *NeQuick G*, while its computational complexity is highly reduced.

Ionosphere's physical behavior is, however, such that one cannot produce an algorithm, which will systematically deliver fully satisfactory compensation of ionospheric error under all conditions. The European Commission (EC), the European Space Agency (ESA), the author(s) or contributor(s) therefore do not assume any responsibility whatsoever for its use, and do not make any guarantee, expressed or implied, about the quality, reliability, fitness for any particular use or any other characteristic of the algorithm. Under no circumstances shall EC, European Union (EU), ESA, the author(s) or contributor(s) be liable for damages resulting directly or indirectly from the use, misuse or inability to use the algorithm.

Acknowledgements

The *NTCM G* electron density model was developed by the German Aerospace Center (DLR). The validation of *NTCM G* single-frequency ionospheric correction algorithm has been performed by DLR with the support of ESA, and the Joint Research Centre (JRC) of the European Commission. The step-by-step algorithmic description of *NTCM G* for Galileo contained in this document and its implementation in different programming languages (Matlab, Simulink, and C/C++) have been a collaborative effort of DLR and JRC. The source codes of the algorithm are available at the website of the European GNSS Service Centre (GSC) (https://www.gsc-europa.eu/).

Document Change Record

Reason for Change	Issue	Revision	Date
First Issue	Issue 1	0	May 2022

Table of Contents

List of Figures

List of Tables

1. Introduction

1.1 Document Scope

This document describes in detail an algorithm to compute ionospheric corrections based on the broadcast coefficients in the navigation message for Galileo[i] single-frequency users, called *NTCM G* (Neustrelitz Total Electron Content Model). This document also includes the guidelines for its implementation in user receivers, and data for the verification of independent implementations.

NTCM G is proposed as an alternative to the reference algorithm *NeQuick G* described in [2].

The reduced complexity and runtime of the *NTCM G* algorithm are considered beneficial, in particular in those user-segments where the user equipment has limited resources available. This is typically the case of the receivers used in civil aviation (e.g., avionics receivers), and location-based services (e.g., smartphones, smartwatches, UAV, IoT devices).

A reference implementation of the *NTCM G* can be found on the website of the European GNSS Service Centre (https://www.gsc-europa.eu/).

1.2 Background

Galileo is the European global navigation satellite system providing a highly accurate and global positioning service under civilian control. Galileo, and in general current GNSS, are based on the broadcasting of electromagnetic ranging signals in the L frequency band. Those satellite signals suffer from a number of undesired effects when propagating through the Earth's atmosphere. In this sense, Earth's atmosphere can be subdivided into:

- the troposphere, whose main effect is a group delay on the navigation signal due to water vapour and the gas components of the dry air. This delay, for microwave frequencies, is non-dispersive (independent of frequency).

- the ionosphere, which is the ionised part of the atmosphere, inducing a dispersive group delay that is several orders of magnitude larger than the one from the

[i] The term "Galileo" is used to refer to the system established under the European GNSS (Galileo) program.

troposphere. Other ionospheric effects such as scintillations may be also observed.

The ionosphere is a region of weakly ionised gas in the Earth's atmosphere lying between about 50 kilometers up to several thousand kilometers from the Earth's surface. Solar radiation is responsible for this ionisation producing free electrons and ions. The ionospheric refractive index (the ratio between the speed of propagation in the media and the speed of propagation in vacuum) is related to the number of free electrons through the propagation path.

Ionospheric electron density and in general ionospheric effects depend on different factors such as time of the day, location, season, solar activity and the interaction between solar activity and the Earth's magnetic field or level of disturbance of the ionosphere, such as those happening during geomagnetic storms. On a large time-scale, solar activity follows a periodic 11-year cycle. The level of solar activity (and hence the solar cycle) is usually represented by solar indices such as the Sun Spot Number (SSN) or the solar radio flux at 10.7 cm (F10.7). The equatorial anomaly regions, located at around ±15-20 degrees on either side of the geomagnetic equator, usually present the largest TEC values. Mid-latitude regions daytime TEC values are usually less than half the value found in the equatorial anomaly region. Polar and auroral regions present moderate TEC values, but larger variability than in mid-latitudes due to the characteristics of the geomagnetic field.

The ionosphere is classically sub-divided in layers characterized by different properties: *D*, *E*, *F*1 and *F*2, the latter being largely responsible for the ionospheric effects which typically affect GNSS applications.

In a first order approximation, the ionospheric propagation delay is inversely proportional to the square of the signal frequency and directly proportional to the integral of the electron density along the ray path, called total electron content (TEC), and given by:

$$d_{Igr} = \frac{K}{f^2} \cdot \int_{path} N \cdot dl \approx \frac{40.3}{f^2} \cdot STEC \qquad \text{Eq. 1}$$

Where d_{Igr} is the ionospheric group delay [m], *f* is the signal frequency [Hz], *N* is the electron density [electrons/m^3], *STEC* [electrons/m^2] is the Slant Total Electron Content, which is commonly expressed in TECU, where 1 TECU equals 10^{16} [electrons/m^2], *path* is the propagation path between receiver and satellite, and the

constant 40.3 is given in [m^3/s^2/electrons]. The ionospheric effect introduces ranging errors of up to several meters, if not adequately corrected. Higher order terms are also present, but they can be usually neglected since they are orders of magnitude smaller (e.g. at Galileo E1 frequency, higher order terms are usually smaller than 20 cm). Please refer to [4] for a full characterization of the ionospheric propagation delay including higher order terms.

The effect induced by the ionosphere on the carrier phase has the same magnitude as the one in the code delay, but opposite sign, meaning that the carrier phase is advanced while propagating through the ionosphere.

Single frequency Galileo users are able to counteract the errors introduced by the ionospheric propagation delay using the *NeQuick G* single-frequency ionospheric correction algorithm described in [2]. Substantial effort has been devoted to reduce the computational load of the NeQuick algorithm and to increase its computational speed [5]. While keeping on working to improve the efficiency of the *NeQuick G* implementation, it has been deemed appropriate to present to users the possibility to use the alternative *NTCM G*, presented in this document.

1.3 NTCM G model

NTCM is an empirical model [6]-[10],[17]) that provides a practical and a cost-effective solution for the determination of global TEC. It makes use of 12 model coefficients, few empirically fixed parameters, and the solar radio flux F10.7 index.

NTCM has been adapted to operate with the broadcast Galileo Effective Ionisation Level coefficients. For this purpose, the F10.7 index is replaced by a particular realization of the Effective Ionisation Level, called $Azpar$ hereafter, which is computed using the three Effective Ionisation Level coefficients broadcast in the navigation message, i.e., (a_{i0}, a_{i1}, a_{i2}) [1]. Although these coefficients were optimized for *NeQuick G*, their applicability to operate the NTCM has been demonstrated [10]. The investigation shows that the *NTCM G* can be successfully driven by the Galileo broadcast Effective Ionisation Level coefficients. The global and regional performance analysis with reference VTEC data provided from the International GNSS Service (IGS), and the Center for Orbit Determination in Europe (CODE)[ii], and from independent Jason-2 data[iii], shows that the performance of *NTCM*

[ii] Reference VEC maps were provided by IGS in form of Global Ionospheric Maps (GIMs). IGS GIMs are obtained from the combination of GIMs provided by the different IGS Ionosphere Associate Analysis Centres (IAACs).

[iii] Jason-2 data was provided by NOAA's National Center for Environmental Information (NCEI).

G was similar to the one obtained using *NeQuick G* model in the global average. A comparison with reference STEC data shows that there is no significant difference in performance between the two models in terms of residual statistics such as Root Mean Square (RMS), mean and Standard Deviation (STD). Please refer to Section 6.1 for additional details on the statistical analysis.

The *NTCM G* algorithm described herein, and the *NeQuick G* algorithm described in [2], are both fully consistent with the Galileo broadcast coefficients.

A global VTEC map, obtained with *NTCM G* considering an $Azpar = 57.5665$ on 15th April 2021 at 14:00 UTC, is illustrated in Figure 1.

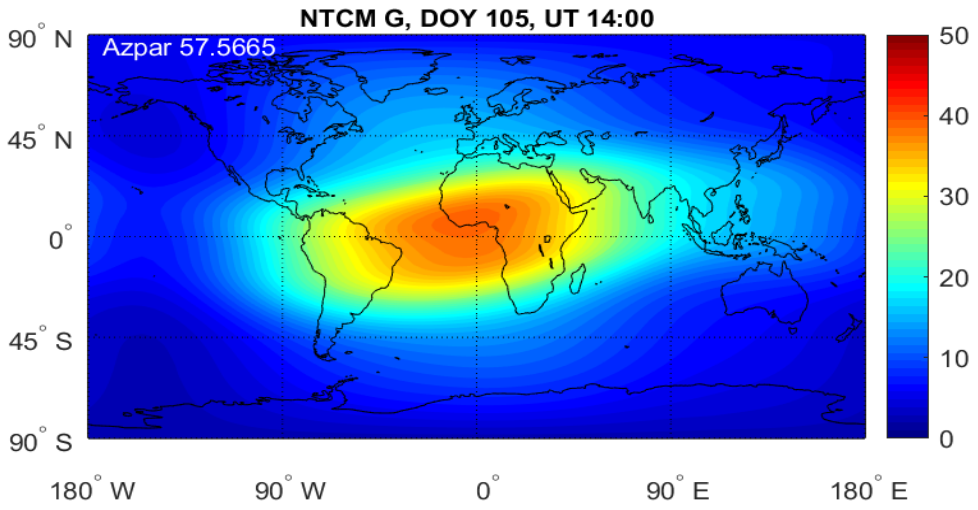

Figure 1. Example of a global VTEC map (in TECU) obtained with *NTCM G*

2.1 Overview

Galileo receivers operating in single frequency mode may use the ionospheric correction algorithm described herein to estimate the ionospheric delay as described in the Step-by-step procedure in Section 2.2. The input parameters required by the algorithm are listed in Section 2.3. The computation of the integrated Vertical TEC (VTEC) is obtained using *NTCM G* driven by the Effective Ionisation Level, $Azpar$, as described in Section 2.4. Finally, Section 2.5 contains the description of the modules to compute the auxiliary parameters required for the derivation of VTEC and the final computation of STEC.

$Azpar$ is used as a proxy measure of the solar activity level [10], and it is determined as follows:

$$Azpar = \left| \sqrt{(a_{i0}^2 + 1633.33 a_{i1}^2 + 4802000 a_{i2}^2 + 3266.67 a_{i0} a_{i2})} \right| \qquad \text{Eq. 2}$$

where (a_{i0}, a_{i1}, a_{i2}) are the three Effective Ionisation Level coefficients broadcast in the Galileo navigation message. The $Azpar$ expression, given in Eq. 2, has been analytically derived based on a best-fit approach using as input the Effective Ionisation Level coefficients broadcast by Galileo during the 2013-2017 period.

2.2 Step-by-step procedure

In order to implement the ionospheric algorithm for Galileo single frequency receivers the following steps shall be followed:

for each satellite-user line-of-sight

Obtain estimates of user receiver position $(\varphi_u, \lambda_u, h_u)$, satellite position $(\varphi_s, \lambda_s, h_s)$ and Universal Time (UT), in terms of time of day and month

Obtain *Effective Ionisation Level* $Azpar$ and broadcast coefficients (a_{i0}, a_{i1}, a_{i2})

Calculate satellite elevation (*E*) and azimuth (*A*) angles

Calculate ionospheric pierce point location $(\varphi_{pp}, \lambda_{pp})$ for the user-to-satellite link at 450 km height as described in Section 2.5.3

Call NTCM G to calculate VTEC at pierce point location $(\varphi_{pp}, \lambda_{pp})$ as described in Section 2.4 and local time (LT) as described in Section 2.5.4.

Calculate ionospheric Mapping Function (MF) using the equation provided in Section 2.5.8.

Convert VTEC to STEC using the ionospheric mapping function.

Convert STEC to time delay using Eq. 1 for the corresponding frequency to obtain the correction

Apply correction to selected link

End

2.3 Inputs and Outputs

In order to calculate VTEC values the algorithm needs as inputs:

Parameter	Description	Unit
a_{i0}	Effective Ionisation Level 1st order parameter	sfu[iv]
a_{i1}	Effective Ionisation Level 2nd order parameter	sfu/deg
a_{i2}	Effective Ionisation Level 3rd order parameter	sfu/deg^2
φ_u	User receiver Geodetic latitude	radians
λ_u	User receiver Geodetic longitude	radians
h_u	User receiver Geodetic height	meters
φ_s	Satellite Geodetic latitude	radians
λ_s	Satellite Geodetic longitude	radians
h_s	Satellite Geodetic height	meters
UT	Universal time	hours
doy	Day of Year (numerical value, 1st January = 1, 1st February=32, …)	dimensionless

Table 1. Input Parameters

*Remark: User r*eceiver and satellite positions estimated values are given in WGS-84 ellipsoidal coordinates: geodetic latitude, geodetic longitude and ellipsoidal height.

The output of the algorithm is VTEC in TECU, that can be converted first to STEC using Eq. 16, and then in ionospheric delay using Eq. 1.

[iv] Note that 'sfu' (solar flux unit) is not a SI unit but can be converted as: 1 sfu = 10^{-22} W m^{-2} Hz^{-1}.

2.3.1 Galileo broadcast ionospheric model parameters

As described in the Galileo OS SIS ICD [1], the following parameters are broadcast in the Galileo navigation message (the parameters are sent within both F/NAV and I/NAV messages):

- Effective Ionisation Level parameters: a_{i0}, a_{i1}, and a_{i2}.
- Ionospheric Disturbance Flags for Regions 1 to 5 (SF_1, SF_2, SF_3, SF_4 and SF_5)[v].

As detailed in the OS SIS ICD [1], the ionospheric correction parameters are transmitted within F/NAV Page Type 1 and I/NAV Word Type 5.

2.4 NTCM G ionospheric Total Electron Content model

The *NTCM G* is an empirical model that allows easy determination of global TEC. The model describes the main ionospheric features with good quality using a small number of model coefficients and parameters. The non-linear approach needs only 12 coefficients and a few empirically fixed parameters for describing the broad spectrum of TEC variation for all levels of solar activity. The computation of the integrated VTEC using the *NTCM G* is presented next.

2.4.1 Computation of VTEC

As described below, the basic modelling approach considers five major dependencies of TEC, i.e., local time dependency (F_1), seasonal dependency (F_2), geomagnetic field dependency (F_3), equatorial anomaly dependency (F_4) and solar activity dependency (F_5). The dependencies are combined in a multiplicative way as:

$$VTEC_{NTCM-G} = F_1 \cdot F_2 \cdot F_3 \cdot F_4 \cdot F_5 \qquad \text{Eq. 3}$$

The main dependencies of VTEC are described by the factors F_i which contain explicitly the model functions and coefficients. The different model functions, F_i, are presented next. The quantities k_1 to k_{12} used in the following equations are model coefficients and their values are given in Table 3.

Local time dependency: F_1

The variation with local time (LT in hours) is separated into diurnal (D), semi-diurnal (SD) and ter-diurnal (TD) harmonic components. The model function describing the local time variation of VTEC, is given by

$$F_1 = cos\chi^{***} + cos\chi^{**}(k_1 cosV_D + k_2 cosV_{SD} + k_3 sinV_{SD} + k_4 cosV_{TD} + k_5 sinV_{TD}) \qquad \text{Eq. 4}$$

[v] The Ionospheric Disturbance Flags SF1 to SF5 are currently not used and reserved for future use.

Where χ is the solar zenith angle. The angular phases of the diurnal (V_D), semi-diurnal (V_{SD}). and ter-diurnal (V_{TD}) variations are defined, respectively by

$$V_D = \frac{2\pi(LT - LT_D)}{24} \quad \text{Eq. 5}$$

$$V_{SD} = \frac{2\pi LT}{12} \quad \text{Eq. 6}$$

$$V_{TD} = \frac{2\pi LT}{8} \quad \text{Eq. 7}$$

in which $LT_D = 14$ hours is the phase shift and LT is the local time in hours computed as indicated in Section 2.5.4.

An approximate 2 hours' delay has been found in the response of the ionospheric/thermospheric system to the daily solar excitation [6]. The investigation shows that the daily maximum of TEC occurs at 14 LT, instead of at 12 LT, for most cases. Therefore, a phase shift LT_D = 14 hours is considered in Eq. 5. The solar zenith angle χ dependency is considered by two functions $cos\chi^{**}$ and $cos\chi^{***}$ and their calculation is given in Section 2.5.6. The Eq. 30 in Section 2.5.6 indicates that cosχ** = 0 at geographic poles, i.e., at φ_{pp} = 90°. This makes the contribution of diurnal, semi-diurnal and ter-diurnal terms in Eq. 4 equal to zero. To avoid such a situation, we introduce an additional term, cosχ***, in Eq. 4.

Seasonal dependency: F_2

The seasonal variation of VTEC is modelled by two components: the annual (A) and the semi-annual (SA) variations through the following expression.

$$F_2 = 1 + k_6 cos(V_A) + k_7 cos(V_{SA}) \quad \text{Eq. 8}$$

In which

$$V_A = \frac{2\pi(doy - doy_A)}{365.25} \quad \text{Eq. 9}$$

$$V_{SA} = \frac{4\pi(doy - doy_{SA})}{365.25} \quad \text{Eq. 10}$$

Where the phase shifts with respect to the beginning of the year are found to be $\mathrm{doy_A} = 18$ days and $\mathrm{doy_{SA}} = 6$ days for the annual and semi-annual variation, respectively, and doy is the day of year.

Geomagnetic field dependency: F_3

VTEC shows a marked correlation with the geomagnetic field resulting in a specific behavior [11], [12]. The geomagnetic field dependency is driven by the geomagnetic latitude φ_m.

$$F_3 = 1 + k_8 cos(\varphi_m) \quad \text{Eq. 11}$$

Where φ_m is the geomagnetic latitude in the IPP in radians. The geomagnetic latitude is generally based on a simple dipole representation of the Earth's magnetic field (see Section 2.5.7).

Equatorial anomaly dependency: F_4

The latitudinal distribution of the TEC shows a minimum at the geomagnetic equator and two maxima appear on both sides of the equator near magnetic latitudes 15 to 20 degrees North and 15 to 20 degrees South. This phenomenon is called equatorial or Appleton anomaly and has been studied by many authors ([12], [13], [14] and [15]). In the *NTCM G* the two ionisation crests are modelled by the following expression:

$$F_4 = 1 + k_9 exp(EC_1) + k_{10} exp(EC_2) \quad \text{Eq. 12}$$

In which

$$EC_1 = -\frac{(\varphi_m - \varphi_{c1})^2}{2\sigma_{c1}^2} \quad \text{Eq. 13}$$

$$EC_2 = -\frac{(\varphi_m - \varphi_{c2})^2}{2\sigma_{c2}^2} \quad \text{Eq. 14}$$

Where $\varphi_{c1} = 16°\text{N}$ is the northward crest, $\varphi_{c2} = -10°\text{N}$ is the southward crest, $\sigma_{c1} = 12°$ and $\sigma_{c2} = 13°$ are best-fit values, and φ_m is the geomagnetic latitude in degrees.

Solar activity dependency: F_5

The strong solar activity dependence of the TEC is formulated by

$$F_5 = k_{11} + k_{12} Azpar \quad \text{Eq. 15}$$

where $Azpar$ is the Effective Ionisation Level in solar flux units (1 flux units = 10^{-22} W m^{-2} Hz^{-1}). The quantity $Azpar$ is computed from the Effective Ionisation Level coefficients and given by Eq. 2.

Equations 3 to 15 give the NTCM formulations and show that the model computes VTEC by multiplying functions from F_1 to F_5.

2.4.2 Constants used

For the calculation of the STEC, some constant parameters are used. They are summarized in Table 2.

Symbol	Constant description	Value	Units
R_e	Earth mean radius	6371.0	km
h_I	Ionospheric Pierce Point height	450.0	km
π	Ratio of a circle's circumference to its diameter	3.1415926535898	dimensionless
Φ_{GNP}	latitude of the geomagnetic North pole	79.74	deg
λ_{GNP}	longitude of the geomagnetic North pole	-71.78	deg

Table 2. Constants' definition

2.4.3 Model coefficients

The main dependencies of TEC are described by the factors F_i which contain explicitly the model functions and coefficients. The quantities k_1 to k_{12} in Eq. 4, Eq. 8, Eq. 11, Eq. 12, and Eq. 15, are model coefficients and their values are given in Table 3.

Symbol	Value
k_1	0.92519
k_2	0.16951
k_3	0.00443
k_4	0.06626
k_5	0.00899
k_6	0.21289
k_7	-0.15414
k_8	-0.38439
k_9	1.14023
k_{10}	1.20556
k_{11} [TECU]	1.41808
k_{12} [TECU/sfu]	0.13985

Table 3. Values of *NTCM G* coefficients

2.5 Auxiliary parameters and STEC computation

To implement the step-by-step procedure described in 2.2 and to compute the *NTCM G* electron density model, several auxiliary parameters are evaluated through specific modules. In the following sections the formulation of each of these modules resulting in the auxiliary parameters is given. Finally, the computation of STEC is presented in Section 2.5.9.

2.5.1 Geodetic to Cartesian coordinates

This module converts geodetic WGS84 coordinates to ECEF.

Inputs:

- geodetic (WGS84) latitude φ [radians],
- geodetic longitude λ [radians],
- geodetic height h [meters],
- Earth's semi-major axis (equatorial radius) a [meters]
- eccentricity of the ellipsoid e [dimensionless]

Output:

- Earth Centred Earth Fixed (ECEF) coordinates (X, Y, Z) [meters]

Geodetic coordinates latitude φ, longitude λ, and height h can be converted into ECEF coordinates (X, Y, Z) using the following equations:

$$X = (N(\varphi) + h) \cdot cos(\varphi) \cdot cos(\lambda) \quad \text{Eq. 16}$$

$$Y = (N(\varphi) + h) \cdot cos(\varphi) \cdot sin(\lambda) \quad \text{Eq. 17}$$

$$Z = (N(\varphi) \cdot (1 - e^2) + h) \cdot sin(\varphi) \quad \text{Eq. 18}$$

$$N(\varphi) = \frac{a^2}{\sqrt{a^2 cos^2(\varphi) + b^2 sin^2(\varphi)}} = \frac{a}{\sqrt{1 - e^2 sin^2(\varphi)}} \quad \text{Eq. 19}$$

where $a = 6378137.0\,[\mathrm{m}]$ is the equatorial radius (semi-major axis) and $b = 6356752.3142\,[\mathrm{m}]$ is the polar radius (semi-minor axis), and $e = \sqrt{1 - \frac{b^2}{a^2}}$ is the eccentricity of the ellipsoid.

2.5.2 Satellite elevation and azimuth angles

This module computes the satellite azimuth and elevation angles.

Inputs:

- user Receiver location in ECEF coordinates (X_u, Y_u, Z_u) [meters],
- satellite location in ECEF coordinates (X_s, Y_s, Z_s) [meters],
- user Receiver latitude φ_u [radians],
- user Receiver longitude λ_u [radians],

Outputs:

- satellite elevation E [radians]
- satellite azimuth A [radians]

$$\begin{bmatrix}\Delta x\\ \Delta y\\ \Delta z\end{bmatrix} = \begin{bmatrix}X_s - X_u\\ Y_s - Y_u\\ Z_s - Z_u\end{bmatrix} \qquad \text{Eq. 20}$$

$$\begin{bmatrix}Dx\\ Dy\\ Dz\end{bmatrix} = \begin{bmatrix}-sin(\varphi_u)\cdot cos(\lambda_u) & -sin(\varphi_u)\cdot sin(\lambda_u) & cos(\varphi_u)\\ -sin(\lambda_u) & cos(\lambda_u) & 0\\ cos(\varphi_u)\cdot cos(\lambda_u) & cos(\varphi_u)\cdot sin(\lambda_u) & sin(\varphi_u)\end{bmatrix}\begin{bmatrix}\Delta x\\ \Delta y\\ \Delta z\end{bmatrix} \qquad \text{Eq. 21}$$

Azimuth angle A can be determined as

$$A = \begin{cases} arctan\left(\frac{Dy}{Dx}\right) & if\ A \geq 0 \\ arctan\left(\frac{Dy}{Dx}\right) + 2\pi & if\ A < 0 \end{cases} \quad \text{Eq. 22}$$

Elevation angle E can be determined as

$$E = \left(0.5 - \frac{arctan\left(\sqrt{Dx^2 + Dy^2}\,/\,Dz\right)}{\pi}\right) \cdot \pi \quad \text{Eq. 23}$$

2.5.3 Ionospheric pierce point latitude and longitude

This module computes the geographic latitude and longitude of the Ionospheric Pierce Point (IPP).

Inputs:

- satellite elevation E [radians],
- satellite azimuth A [radians]
- user receiver latitude φ_u [radians],
- user receiver longitude λ_u [radians],
- ionospheric shell height h_I [km],
- Earth's radius R_e [km]

Outputs:

- pierce point latitude φ_{pp} [radians],
- pierce point longitude λ_{pp} [radians]

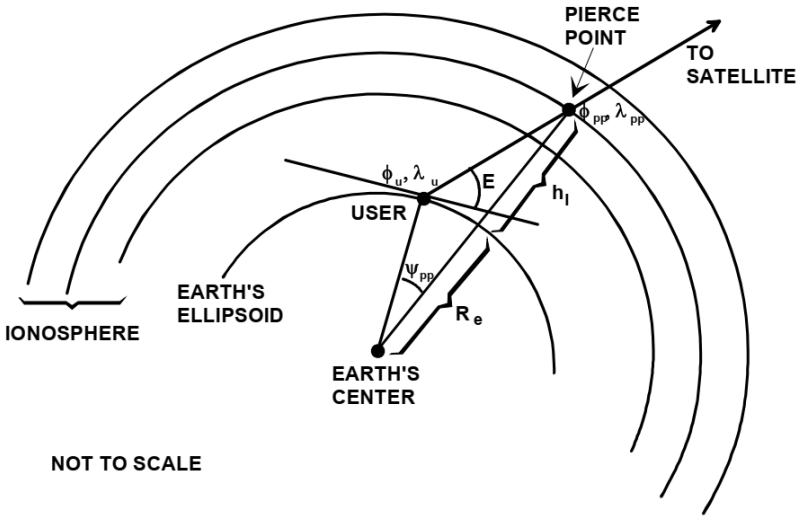

Figure 2. Ionospheric pierce point geometry (reprinted from RTCA MOPS DO-229 [3])

Calculate the Earth's central angle ψ_{pp} between the user position and the Earth projection of the pierce point [radians]

$$\psi_{pp} = \frac{\pi}{2} - E - arcsin\left(\frac{R_e}{(R_e + h_I)} cos(E)\right) \quad \text{Eq. 24}$$

Calculate pierce point latitude φ_{pp} [radians]

$$\varphi_{pp} = arcsin\Big(sin(\varphi_u) \cdot cos(\psi_{pp}) + cos(\varphi_u) \cdot sin(\psi_{pp}) \cdot cos(A)\Big) \quad \text{Eq. 25}$$

Calculate pierce point longitude λ_{pp} [radians]

$$\lambda_{pp} = \lambda_u + arcsin\left(\frac{sin(\psi_{pp}) \cdot sin(A)}{cos(\varphi_{pp})}\right) \quad \text{Eq. 26}$$

2.5.4 Local time

This module computes the local time LT given the pierce point longitude and UT.

Inputs:

- pierce point longitude λ_{pp} [radians],

- Universal Time UT [hours and decimals].

Output:

- local time LT [hours and decimals]

$$LT = UT + \frac{\left(\lambda_{pp} \cdot \frac{180}{\pi}\right)}{15} \qquad \text{Eq. 27}$$

2.5.5 Sun's declination

This module computes the Sun's declination for the applicable day.

Input:

- Day of Year (doy)

Output:

- Sun's declination δ [radians].

$$\delta = 23.44 \cdot sin(0.9856 \cdot (doy - 80.7) \cdot \pi/180) \cdot \pi/180 \qquad \text{Eq. 28}$$

2.5.6 Solar zenith angle dependence

This module computes the dependency of TEC with the solar zenith angle χ , i.e., cosχ** and cosχ*** used in Eq. 4.

Inputs:

- pierce point latitude φ_{pp} [radians],
- Sun's declination δ [radians]

Outputs:

- solar zenith angle dependence term $cos\chi^{**}$ [dimensionless]
- solar zenith angle dependence term $cos\chi^{***}$ [dimensionless]

The solar zenith angle χ dependency is considered by the following expressions:

$$cos\chi^{***} = cos\left(\varphi_{pp} - \delta\right) + P_{F1} \quad \text{Eq. 29}$$

$$cos\chi^{**} = cos\left(\varphi_{pp} - \delta\right) - \frac{2}{\pi} \cdot \varphi_{pp} \cdot sin\delta \quad \text{Eq. 30}$$

where $P_{F1} = 0.4$, φ_{pp} is the geographic latitude and δ is the declination of the sun (all angles in radians). The value P_{F1} in Eq. 29 is chosen in such a way that the term $cos\chi^{***}$ has always a positive contribution.

2.5.7 Geographic to geomagnetic latitude

This module computes the geomagnetic latitude φ_m of the pierce point based on a magnetic dipole model.

Inputs:

- pierce point latitude φ_{pp} [radians],
- pierce point longitude λ_{pp} [radians],
- latitude of the geomagnetic North pole Φ_{GNP} [radians],
- longitude of the geomagnetic North pole λ_{GNP} [radians]

Output:

- geomagnetic latitude φ_m [radians].

$$\varphi_m = arcsin\left(sin\left(\varphi_{pp}\right) \cdot sin(\Phi_{GNP}) + cos\left(\varphi_{pp}\right) \cdot cos(\Phi_{GNP}) \cdot cos\left(\lambda_{pp} - \lambda_{GNP}\right)\right) \quad \text{Eq. 31}$$

2.5.8 Mapping function

This module computes the MF used to convert the estimated VTEC to STEC.

Inputs:

- Earth's radius R_e [km],
- pierce point height h_I [km],

- satellite elevation angle E [radians],

Output:

- Modified Single Layer Model mapping function, MF_{MSLM} [dimensionless]

The Modified Single Layer Model (MF_{MSLM}) in [16] is used for the conversion of VTEC to STEC.

$$MF_{MSLM} = \frac{1}{\sqrt{1 - (sinz)^2}} \quad \text{Eq. 32}$$

$$sinz = \frac{R_e}{R_e + h_I} sin\left(0.9782 \cdot \left(\frac{\pi}{2} - E\right)\right) \quad \text{Eq. 33}$$

where $R_e = 6371$ [km] is the Earth's mean radius, $h_I = 450$ [km] is the ionospheric pierce point (IPP) height, and E is the satellite elevation angle in radians.

2.5.9 Computation of STEC

NTCM G is a two-dimensional VTEC model and therefore a mapping function (MF) or obliquity factor is needed for the conversion of VTEC to slant TEC (STEC).

$$STEC = MF_{MSLM} \cdot VTEC_{NTCM-G} \quad \text{Eq. 34}$$

Where MF_{MSLM} is a Modified Single Layer Model (MSLM) mapping function and can be computed as described in Section 2.5.8.

3. Implementation Guidelines for User Receivers

This section provides practical guidelines for the implementation of the ionospheric model described in Section 2. within Galileo user receivers.

3.1 Applicability and coherence of broadcast coefficients

In nominal conditions, a Galileo user receiver decoding the Galileo navigation message from *N* Galileo satellites simultaneously, with $N > 1$, would receive at a given epoch, the same broadcast ionospheric coefficients for all *N* satellites. However, when the ionospheric parameters are updated, given that the message up-link to different satellites is not necessarily synchronized due to the need to be within the visibility of an Up-Link Station (ULS) this may not be the case. It may happen that some satellites broadcast the recently updated coefficients while others still broadcast the previous batch of coefficients. In such a situation, a user could take advantage of the GST information broadcast by the satellites to discern the latest set of coefficients broadcast by the system. The receiver will then use the same set of coefficients to compute the ionospheric delay for all *N* satellites in view. Nevertheless, the correction capability will still be achieved, on a statistical sense, independently of the set of parameters adopted (i.e., previous or updated).

3.2 Computation rate of ionospheric corrections

The ionosphere variations in nominal conditions are fairly slow and, for the majority of applications, it is not required to re-compute the delay correction at high rates. In most cases, it may suffice if stationary receivers or pedestrian users compute the corrections every 30 seconds.

4. Annex A - Applicable and Reference Documents

4.1 Applicable Documents

[1] European GNSS (Galileo) Open Service Signal In Space Interface Control Document (OS SIS ICD), Issue 2.0, European Union, January 2021.

[2] European GNSS (Galileo) Open Service—Ionospheric correction algorithm for Galileo single frequency users, Issue 1.2, September 2016, European Commission (EC)

4.2 Reference Documents

[3] Minimal Operational Performance Standards for GPS/WAAS Airborne Equipment, RTCA-DO 229 F, June 11, 2020

[4] Hoque M. M., Jakowski N., "Estimate of higher order ionospheric errors in GNSS positioning," *Radio Science*, vol. 43, no. 5, 2008, doi:10.1029/2007RS003817

[5] Orus-Perez R., Nava B., Kashcheyev A., Grosu A., Scortan S., "Considerations for NeQuick G Speed Optimization", 2nd ed., URSI AT-RASC, Gran Canaria, Spain, 2018.

[6] Jakowski N., Hoque M. M., Mayer C. A., "New global TEC model for estimating transionospheric radio wave propagation errors," *Journal of Geodesy*, 2011, vol. 85, no. 12, pp. 965-974, doi: 10.1007/s00190-011-0455-1

[7] Hoque M. M., Jakowski N., "An Alternative Ionospheric Correction Model for Global Navigation Satellite Systems," *Journal of Geodesy*, vol. 89, no. 4, 2015, pp. 391-406. doi: 10.1007/s00190-014-0783-z. ISSN 0949-7714

[8] Hoque M. M., Jakowski N., Berdermann J., "Ionospheric correction using NTCM driven by GPS Klobuchar coefficients for GNSS applications," *GPS Solution*, vol. 21, no. 4, 2017, pp. 1563-1572, https://doi.org/10.1007/s10291-017-0632-7

[9] Hoque M. M., Jakowski N., Berdermann J.," Positioning performance of the NTCM model driven by GPS Klobuchar model parameters," *Space Weather Space Climate*, Volume 8, A20, 2018, https://doi.org/10.1051/swsc/2018009

[10] Hoque, M. M., Jakowski, N., Orús Pérez, R., "Fast ionospheric correction using Galileo Az coefficients and the NTCM model," *GPS Solutions*, 2019, doi: 10.1007/s10291-019-0833-3

[11] Davies, K. (Ed.) (1990), Ionospheric Radio, Peter Peregrinus Ltd., London, ISBN 978-0863411861.

[12] Jakowski N., Wilken V., Mayer C., "Space weather monitoring by GPS measurements on board CHAMP," Space Weather-the International Journal of Research and Applications, vol. 5, no. 8, 2007, pp. 8006, doi:10.1029/2006SW000271.

[13] Rishbeth, H., Lyon A. J., Peart M., “Diffusion in the equatorial F layer,” *Journal of Geophysical Research*, vol .68, no. 9, 1963, pp. 2559-2569, doi: 10.1029/JZ068i009p02559

[14] Bramley E. N., Peart M., “Diffusion and electromagnetic drift in the equatorial F2 region,” *Journal of Geophysical Research*, vol. 69, no. 21, 1964, pp. 4609–4616, doi: 10.1029/JZ069i021p04609.

[15] Goldberg R. A., Kendall P. C., Schmerling E. R., “Geomagnetic control of electron density in F region ionosphere, *Journal of Geophysical Research*, vol. 69, no. 3, 1964, pp. 417-427

[16] Schaer S., “Mapping and Predicting the Earth’s Ionosphere Using the Global Positioning System,” *Geod.-Geophys. Arb. Schweiz*, Vol. 59, 1999

[17] Hoque M. M., Jakowski N, Osechas O., Berdermann J., "Fast and Improved Ionospheric Correction for Galileo Mass Market Receivers," *Proceedings of the 32nd International Technical Meeting of the Satellite Division of The Institute of Navigation (ION GNSS+ 2019)*, Miami, Florida, September 2019, pp. 3377-3389. https://doi.org/10.33012/2019.17106

[18] Hoque M M., Jakowski N., Cahuasquí J. A., "Fast Ionospheric Correction Algorithm for Galileo Single Frequency Users," *2020 European Navigation Conference (ENC)*, 2020, pp. 1-10, doi: 10.23919/ENC48637.2020.9317502.

[19] Sanz Subirana, J., Juan Zornoza J.M., Hernández-Pajares M., “GNSS Data Processing, Vol. 1: Fundamentals and Algorithms,” *ESA Communications*, ISBN 978-92-9221-886-7

[20] Ibáñez D., Rovira-García A., Sanz J., Juan J. M., Gonzalez-Casado G., Jimenez-Baños D., López-Echazarreta C., Lapin I., “The GNSS Laboratory Tool Suite (gLAB) updates: SBAS, DGNSS and Global Monitoring System,” *9th ESA Workshop on Satellite Navigation Technologies (NAVITEC 2018)*, Noordwijk, The Netherlands. December 5 - 7, 2018. DOI: 10.1109/NAVITEC.2018.8642707

[21] Aragon-Angel A., Rovira-Garcia A., Arcediano-Garrido E., Ibáñez-Segura D., “Galileo Ionospheric Correction Algorithm Integration into the Open-Source GNSS Laboratory Tool Suite (gLAB)”. *Remote Sens.* 2021, 13, 191. https://doi.org/10.3390/rs13020191

[22] Orus, R., “Ionospheric error contribution to GNSS single-frequency navigation at the 2014 solar maximum”. *Journal of Geodesy*, 2017, 91, 397–407. https://doi.org/10.1007/s00190-016-0971-0

[23] Orus Perez, R., Parro-Jimenez, J. M., & Prieto-Cerdeira, R. (2018). Status of NeQuick G after the solar maximum of cycle 24. Radio Science, 53, 257-268, 257-268. https://doi.org/10.1002/2017RS006373

5. Annex B - Acronyms and Definitions

5.1 Acronyms

CDDIS	Crustal Dynamics Data Information System
CODE	Center for Orbit Determination in Europe
DLR	German Aerospace Center
EC	European Commission
ECEF	Earth Centred Earth Fixed
EGNOS	European Geostationary Navigation Overlay Service
ESA	European Space Agency
FOC	Full Operational Capability
GIMs	Global Ionospheric Maps
GIOVE	Galileo In Orbit Validation Element
GNSS	Global Navigation Satellite System
GPS	Global Positioning System
GSS	Galileo Sensor Stations
IAACs	IGS Ionosphere Associate Analysis Centers
IGRF	International Geomagnetic Reference Field
IONEX	Ionosphere Map Exchange format
IoT	Internet of Things
IOV	In Orbit Validation
IPP	Ionospheric Pierce Point
IGS	International GNSS Service
JRC	Joint Research Centre
LT	Local Time
MF	Mapping Function
MOPS	Minimum Operational Performance Standards
MSLM	Modified Single Layer Model
NTCM	Neustrelitz TEC Model

OS	Open Service
PPP	Precise Point Positioning
RINEX	Receiver Independent Exchange
RMS	Root Mean Square
RTCA	Radio Technical Commission for Aeronautics
SBAS	Satellite Based Augmentation System
SINEX	Solution Independent Exchange
SISICD	Signal In Space Interface Control Document
s.f.u.	Solar Flux Unit
SoL	Safety of Life
SPP	Single Point Positioning
SSN	Sun Spot Number
STD	Standard Deviation
STEC	Slant Total Electron Content
TEC	Total Electron Content
TECU	TEC Unit
UAV	Unmanned Aerial Vehicle
ULS	Up-Link Stations
UT	Universal Time
VTEC	Vertical Total Electron Content
WAAS	Wide Area Augmentation System

6. Annex C – Validation of *NTCM G* Performance against *NeQuick G*

In this section, the performance of the proposed *NTCM G* model is compared with that of *NeQuick G*. The source code of *NeQuick G* used for this investigation can be found at the European space software repository of ESA (https://essr.esa.int/project/NeQuickg-galileo-ionospheric-correction-model). It is worth mentioning that this software implementation and the one freely available on the website of the European GNSS Service Centre (https://www.gsc-europa.eu/), provide the exact same results [21] [vi].

The comparisons in Section 6.1 have been done in terms of VTEC and STEC residuals, which are defined as the difference between a reference and its corresponding modelled TECs[vii]. The final combined ground-based VTEC maps (GIMs) from IGS, named IGSG[viii], were used as reference VTEC values. Reference STEC data was computed from RINEX observations collected by over 200 worldwide IGS stations. In Section 6.2 the analysis focuses on the performance of the ionospheric correction algorithms in the position domain. Two analyses have been performed. The first analysis focused on the daily performance obtained at three selected geographic locations representative of high, medium, and low latitude regions. The second analysis considered the 68th, 90th and 95th percentiles of the daily 3D positioning error computed at 47 globally distributed locations. Finally, Section 6.3 validates the *NTCM G* performance over the year 2002. This year is of particular interest since it corresponds to a year with elevated solar activity within the solar cycle 23 and outside the perimeter of the fitting period (within solar cycle 24) used for the derivation of the *NTCM G* empirical parameters. This analysis has been carried out by ESA, which used a network of IGS stations resembling the current Galileo ground network in order to generate the Az parameters driving both the *NTCM G* and *NeQuick G* models.

[vi] The *NeQuick G* implementation available on the European GNSS Service Centre is provided under the European Union Public Licence v1.2. The *NeQuick G* implementation available on ESA repository is provided under the European Space Agency Community License v2.4 Permissive (Type 3).

[vii] The STEC is proportional to the range of errors experienced by a GNSS single frequency user and can be converted to range delay using Eq. 1.

[viii] IGSG are generated from the combination of independently computed GIMs from different IAACs.

6.1 NTCM G performance in the TEC domain

6.1.1 Vertical TEC performance

The IGS VTEC product IGSG is taken as reference datasets for performance comparison. The daily IONEX (ionosphere exchange) files of IGSG data can be downloaded from the NASA's Crustal Dynamics Data Information System (CDDIS) archive. The *NTCM G* and *NeQuick G* model-derived VTECs are computed at each grid location and time step and then compared with the corresponding reference VTEC values.

The model residuals (VTECmodel – VTECigsg) are determined and the corresponding mean, Standard Deviation (STD), and Root Mean Squares (RMS) are computed and enlisted in Table 4 for the years 2014 and 2015. Additionally, considering that ionospheric effects are most dominant in the low latitude region during daytime hours, we also compared the model performance for the low latitude region 30° N – 30° S at daytime hours 06:00-18:00 local time. Results are summarised in Table 5.

Residual error statistics in TECU	NeQuick G		NTCM G	
	2014	2015	2014	2015
global RMS	9.6	7.8	7.8	6.4
global mean	-3.3	-2.7	-1.5	-0.6
global STD	9.0	7.4	7.7	6.4

Table 4. Statistics of model residuals with respect to the reference *IGSG* data showing their performances on a global scale and for a whole day.

Residual error statistics in TECU	NeQuick G		NTCM G	
	2014	2015	2014	2015
regional RMS	17.0	10.7	13.8	9.6
regional mean	-9.1	1.2	-6.8	0.8
regional STD	14.4	10.6	12	9.5

Table 5. Statistics of model residuals with respect to the reference *IGSG* data showing their performances for low latitude region (30° N – 30° S) and daytime (06:00-18:00 local time).

By comparing the values in Table 4 and Table 5, *NTCM G* residual statistics results indicate that *NTCM G* provides accurate corrections, resulting in similar performances as those obtained using *NeQuick G*. Results presented consider both global and regional cases (i.e., low latitude day time) during the years 2014 and 2015.

Figure 3 and Figure 4 show the RMS residuals for *NeQuick G* (left figures) and *NTCM G* (right figures) over the globe for different local times (LT) and for the years 2014 and 2015. Figure 3 shows the error distribution when all local times (0-24 LT) are considered, whereas Figure 4 shows the error distribution for the daytime hours 12-15 LT. In each case, the RMS residuals are determined separately at each grid location (2.5° and 5° latitude and longitude grid, respectively) considering a full year of data.

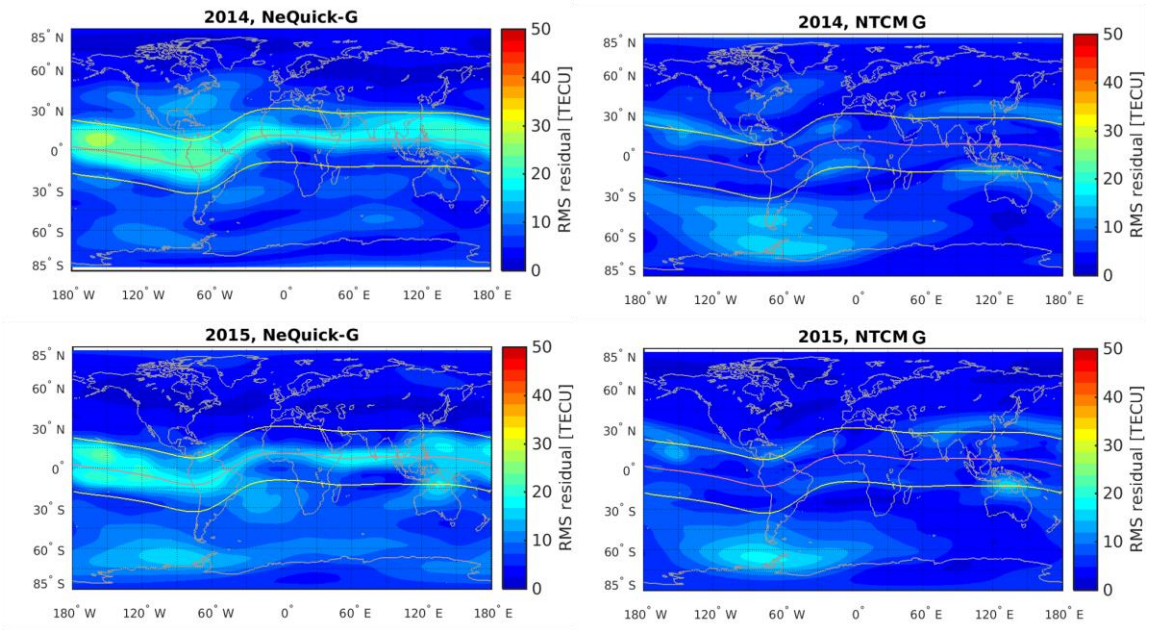

Figure 3. VTEC RMS residual error distribution in 2014 (top panel) and 2015 (bottom panel) for *NeQuick G* (left panel) and *NTCM G* (right panel) considering all local times. Reprinted from [18]

Figure 3 shows that at the equatorial regions, on both sides of the geomagnetic equator, *NeQuick G* results in larger RMS errors when compared to the *NTCM G* model. This is true for both years. However, *NTCM G* shows comparatively larger errors at around 60° S and 60° W geographic regions.

By comparing *NeQuick G* errors in Figure 3 and Figure 4, we see that RMS errors are appreciably higher for the local noon case (12- 15 LT) compared to the all local time case (Figure 3). On the other hand, the *NTCM G* errors resulted to be just slightly increased for the local noon case compared to the all local time case (see Figure 4).

It is worth noting, that the local accuracy and reliability of IGS VTEC products presents geographically unbalances, since it is highly dependent on the coverage (presence of GNSS stations) in a particular region. Continental areas, where the number of available ground stations is high, are in general more reliable and accurate than areas where the number of stations are low, like in the oceanic regions. The large inaccuracies observed in Figure 4 in the pacific area can be partially attributable to a lower accuracy of the reference product. In fact, the magnitude of the expected errors in that region is not confirmed by the positioning results obtained at single stations located in this area and used to derive the results presented in Section 6.2.

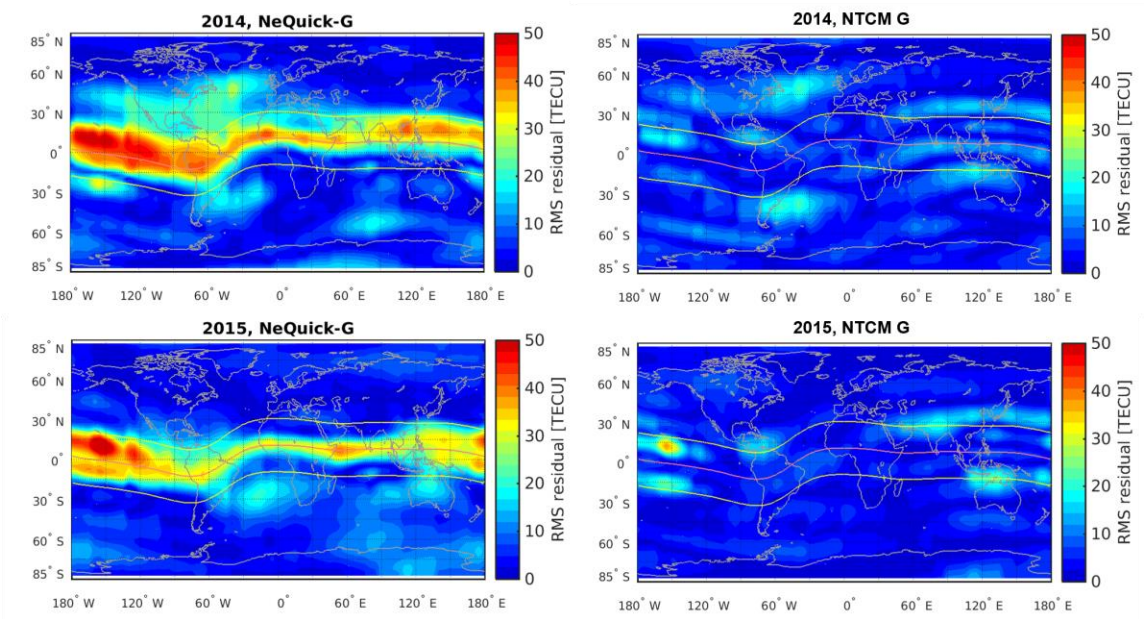

Figure 4. VTEC RMS residual error distribution in 2014 (top panel) and 2015 (bottom panel) for *NeQuick G* (left panel) and *NTCM G* (right panel) considering daytime hours 12-15 LT. Reprinted from [18]

More details on the methodology used and results presented in this section can be found in [18].

6.1.2 Slant TEC performance

The performance of *NTCM G* and *NeQuick G* is also assessed using independent Slant Total Electron Content (STEC) measurements computed at about 120 - 160 worldwide IGS ground stations using GPS SiS measurements and for every day in the periodMarch 2013 to December 2021. The *NTCM G* and *NeQuick G* model-derived STECs are computed at each station location for the same link geometries considering only elevation angles above 5°. The comparisons are done in terms of STEC residual,

which is defined as the difference between the modelled STEC and its corresponding STEC observation (i.e. $STEC_{model}$ - $STEC_{obs}$), on a global scale and the different MODIP bands.

RMS of STEC residuals are computed on a daily basis and over a total of about 10.6 billion samples. The results are plotted in Figure 5.

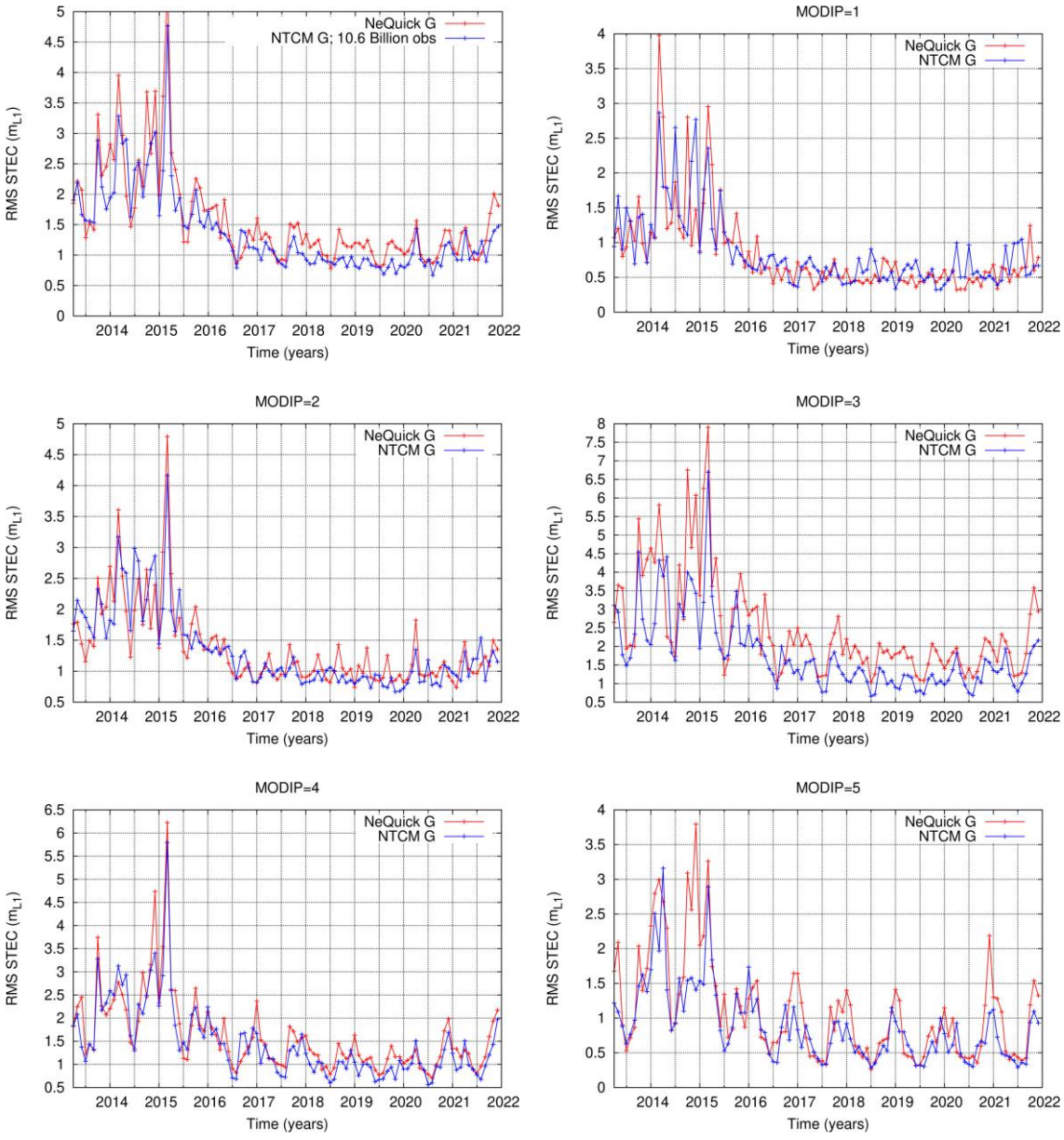

Figure 5. Statistics of daily STEC residuals (monthly average) for the period March 2013 - December 2022 using *NeQuick G* and *NTCM G*. The left upper picture shows the global performance, while the other panels correspond to the different MODIP bands.

By comparing the RMS residual plots in all panels of Figure 5, we see that the performance of both models is very similar and can be concluded that there is no significant difference in performance between *NeQuick G* and *NTCM G*.

More details on the methodology used and results presented in this section can be found in [23].

6.2 NTCM G performance in the Position domain

The performance of the *NTCM G* model in the position domain is compared with the one obtained using *NeQuick G*. The first analysis, presented in Section 6.2.1, focuses on the daily performance obtained at three selected geographic locations representative of high, medium, and low latitude regions. The second analysis, presented in Section 6.2.2, considers the 68th, 90th and 95th percentiles of the daily 3D positioning error averaged over 47 globally distributed locations.

6.2.1 Local 3D Position error

The analysis presented in this section compares the 3D position error obtained using *NTCM G* and *NeQuick G* at three different locations and covering 14 days in both June and December 2004.

Position solutions have been obtained using a standard Single Point Positioning (SPP) approach [19], in which the ionospheric corrections are computed using *NeQuick G* and *NTCM G*. The actual (considered as the "true") 3D user positions are known from the IGS SINEX (Solution Independent Exchange) product and subtracted from each SPP solution to obtain associated position errors. In addition, the actual 3D positions are compared with ionosphere uncorrected SPP solutions. GPS code-pseudorange measurements from RINEX (Receiver Independent Exchange) observation files were used for the computation of the SPP solution. For determining the SPP solution, the gLAB software tool developed by the research group gAGE from the Universitat Politecnica de Catalunya [20], is used. In order to perform the *NTCM G* validation, the *NTCM G* implementation, as well as the *NeQuick G* implementation obtained from the European space software repository of ESA, were integrated into gLAB.

Three geodetic IGS stations were considered as test user positions. The geographic locations of the stations were selected so that they can be considered representative of high, medium and low latitude regions. A high latitude IGS station at HOFN – Iceland (64.27° N, -15.20° E), a middle latitude station at WTZR – Germany (49.14° N, 12.88° E), and a low latitude station at HARB – South Africa (-25.89° N, 27.71° E) were considered. The SPP solutions are computed for two distinct two-week periods: 16th

to 30th of June and 17th to 31st of December 2014 representing Northern hemisphere summer and winter, respectively. The hourly mean and STD of 3D position errors are estimated separately for each model during summer and winter months. Figure 6, Figure 7, and Figure 8 show the diurnal variation of the 3D position error in terms of hourly mean (top panel) and STD variation (bottom panel).

Figure 6 depicts the performance analysis results at a high latitude station. The figure shows that the 3D mean position errors are similar for *NTCM G* (black top-left) and *NeQuick G* (blue top-left) during the summer month (June). During the winter month (December) *NeQuick G* performs slightly better than *NTCM G*. The standard deviation of 3D position errors shows similar trends (see plots in the bottom panel).

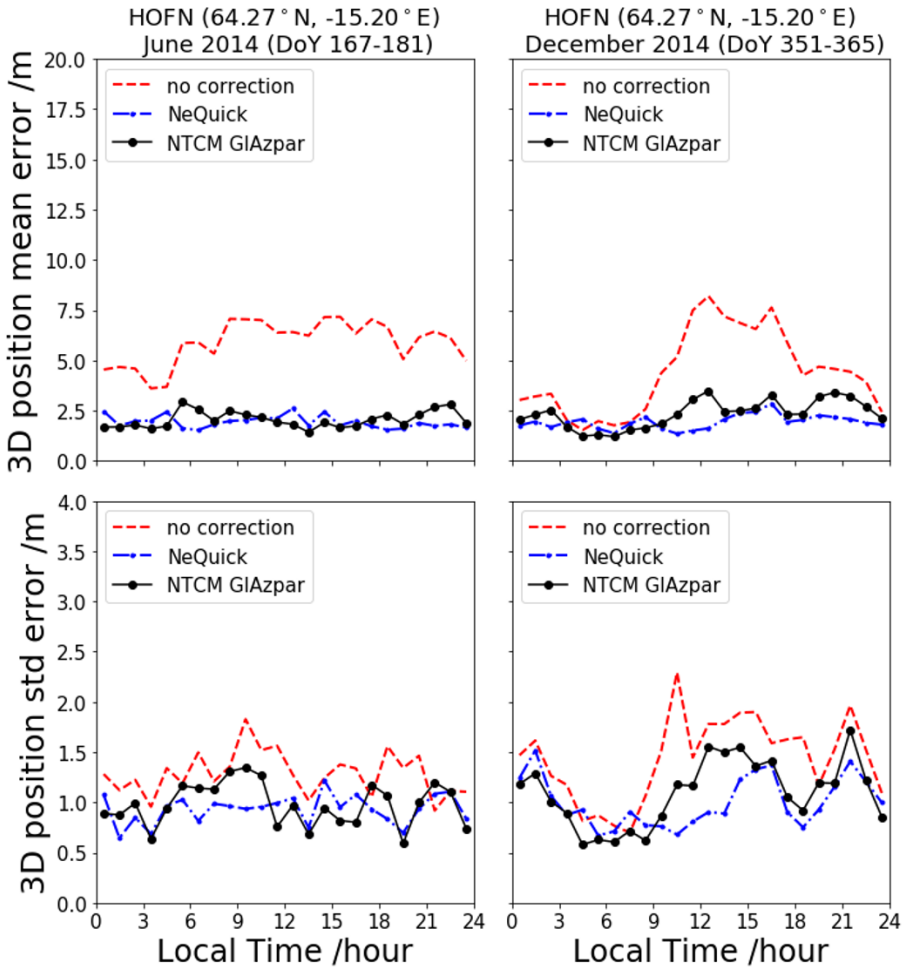

Figure 6. Diurnal variation of the 3D position error for different models at HOFN – Iceland (64.27° N, -15.20° E) in terms of mean (top panel) and STD variation (bottom panel) during 16 - 30 June (left panel) and 17 – 31 December 2014 (right panel). Reprinted from [18].

Figure 7 shows the performance analysis results at a middle latitude station. The 3D mean position errors result to be less for both *NTCM G* and *NeQuick G* compared to the no-correction case.

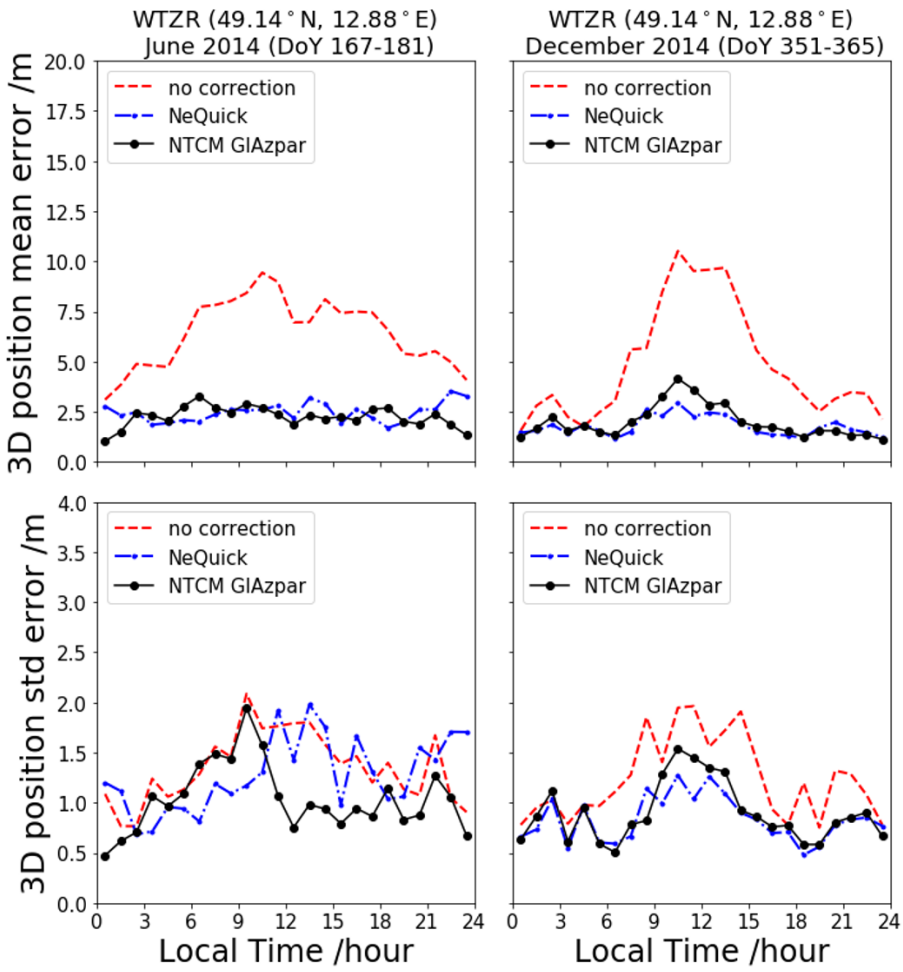

Figure 7. Diurnal variation of the 3D position error for different models at WTZR – Germany (49.14° N, 12.88° E) in terms of mean (top panel) and STD variation (bottom panel) during 16 - 30 June (left panel) and 17 – 31 December 2014 (right panel). Reprinted from [18].

Figure 8 shows the performance analysis results at a low latitude station. During June both models perform very similarly whereas during December *NeQuick G* shows slightly higher 3D mean position errors during daytime hours (e.g., 6-18 LT).

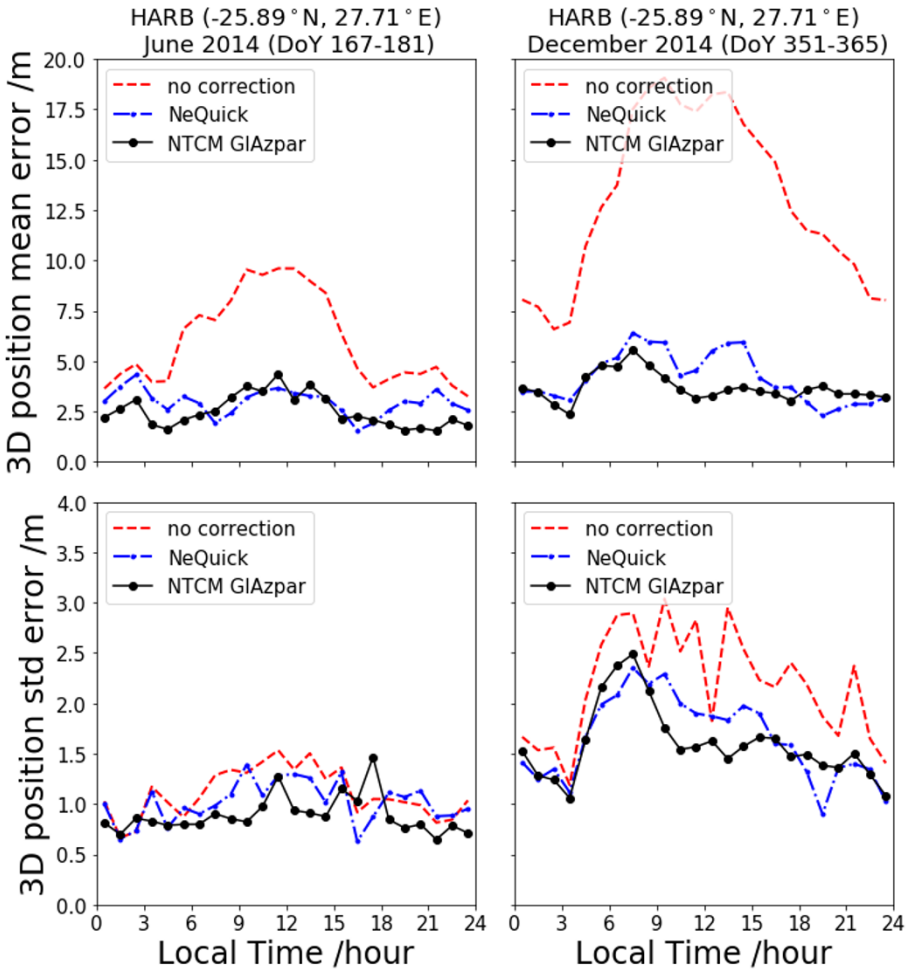

Figure 8. Diurnal variation of the 3D position error for different models at HARB – South Africa (-25.89° N, 27.71° E) in terms of mean (top panel) and STD variation (bottom panel) during 16 - 30 June (left panel) and 17 – 31 December 2014 (right panel). Reprinted from [18].

The results in the position domain show that the *NTCM G* model exhibit excellent performance similar to the one obtained using *NeQuick G*, and this is valid for all the three exemplary locations selected in this analysis.

6.2.2 Global mean of 3D Position error

In this section the analysis on the position performance has been extended and computed at 47 global locations over the whole years 2014 and 2019. Modelling errors, other than the residual ionospheric delay, are drastically reduced by implementing a PPP approach as described in [22], thus allowing for a complementary test of the error contribution due to the mismodelling of the ionosphere.

The following picture shows the location of the 47 IGS stations used for the derivation of the positioning errors. It is worth noting that the availability of each single station varies on a daily basis, therefore the effective number of stations effectively used on each day might be lower than 47.

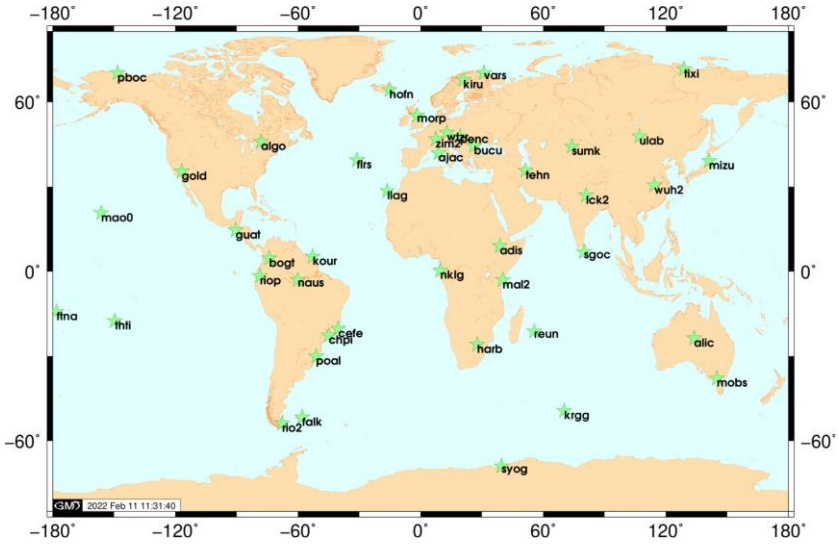

Figure 9. Global set of IGS receivers used for the position domain performance for 2014 and 2019. This example is for day of year 199 of 2014 where 44 receivers are present.

For the performance analysis the 68th, 90th and 95th percentiles are computed for each available station on a daily basis and then a 15-days global average is extracted, weighted by the number of stations available on each day. The following plots show the global mean for the years 2014 and 2019.

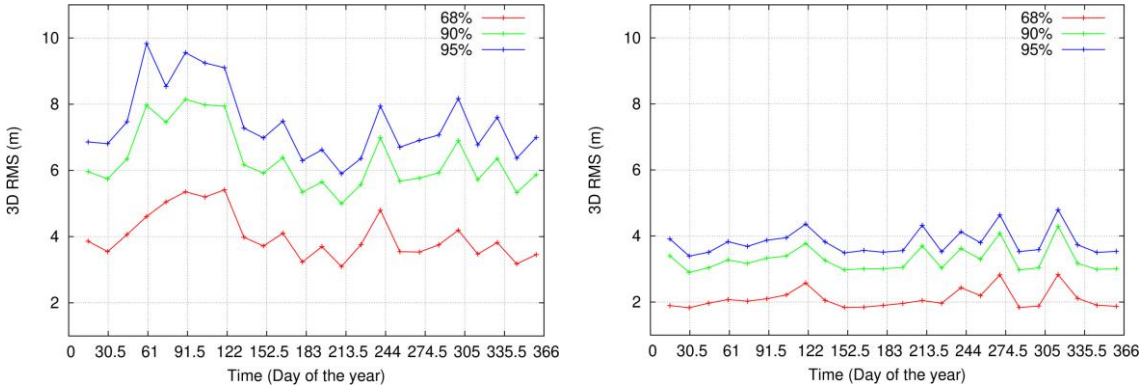

Figure 10. 3D error as a function of the day for different percentiles and years. Left is 2014 and Right is 2019. Notice that the error is the 15-day weighted average.

A comparison between *NTCM G* and *NeQuick G* for the 68% percentile of the 3D positioning error is given in Figure 11. The plot shows that the two models perform in a very similar manner.

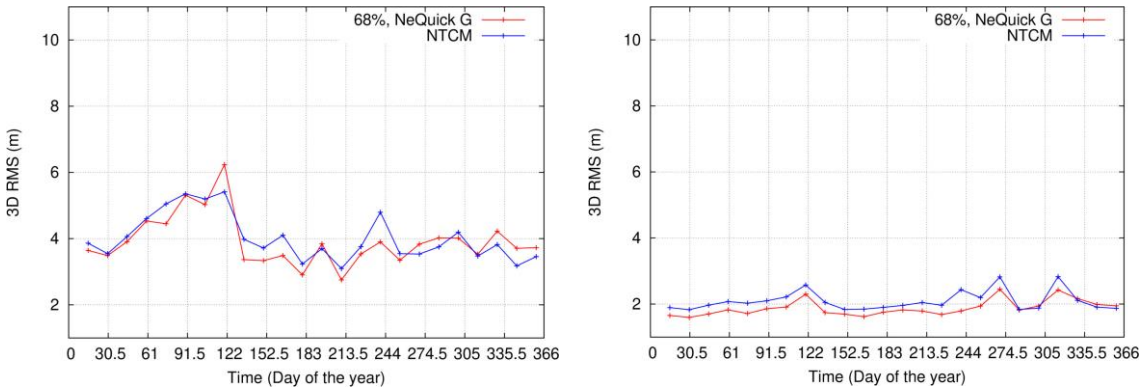

Figure 11. 3D error as a function of the day for 68% percentile and years. Left is 2014 and Right is 2019. Notice that the error is the 15-day weighted average.

6.3 Simulations for 2002 solar maximum conditions

The aim of this section is to assess the behaviour of the *NTCM G* during a time period subject to a particularly high solar activity and outside the fitting period used for the derivation of the *NTCM G* empirical parameters (2013-2017, as reported in [10]). The year 2002, corresponding to a year with particularly elevated solar activity within the solar cycle 23, fulfils both the above conditions and has been selected for the analysis.

Since no Effective Ionisation Level coefficients are available for this period of time[ix], a network of IGS receivers resembling the current Galileo ground network (i.e. by selecting IGS stations closer to the actual GSS) has been used to estimate the broadcast coefficients (a_{i0}, a_{i1}, a_{i2}) driving both the *NTCM G* and the *NeQuick G* models. Figure 12 depicts the location of the selected IGS stations.

[ix] Galileo started broadcasting the Effective Ionisation Level coefficients in March 2013.

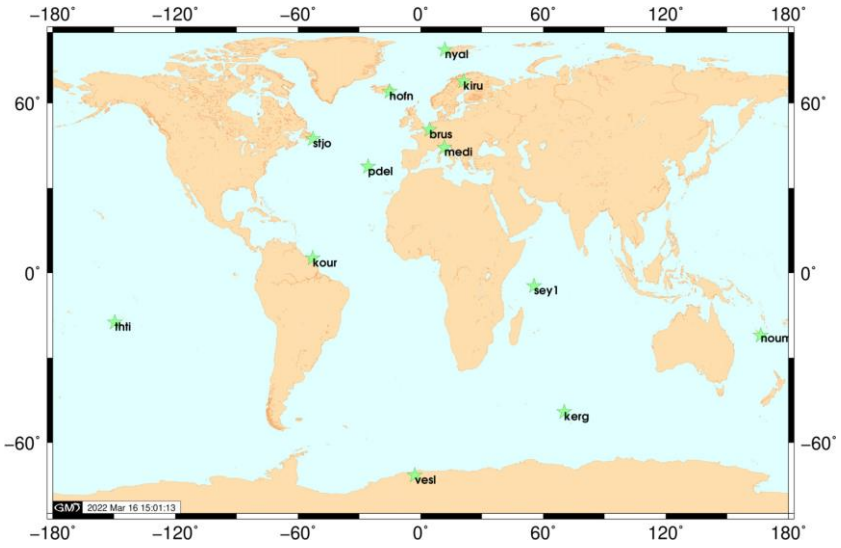

Figure 12. Global set of IGS ground receivers to simulate the GSS network for 2002.

The time series of the estimates of the three broadcast coefficients (a_{i0}, a_{i1}, a_{i2}) is given in Figure 13.

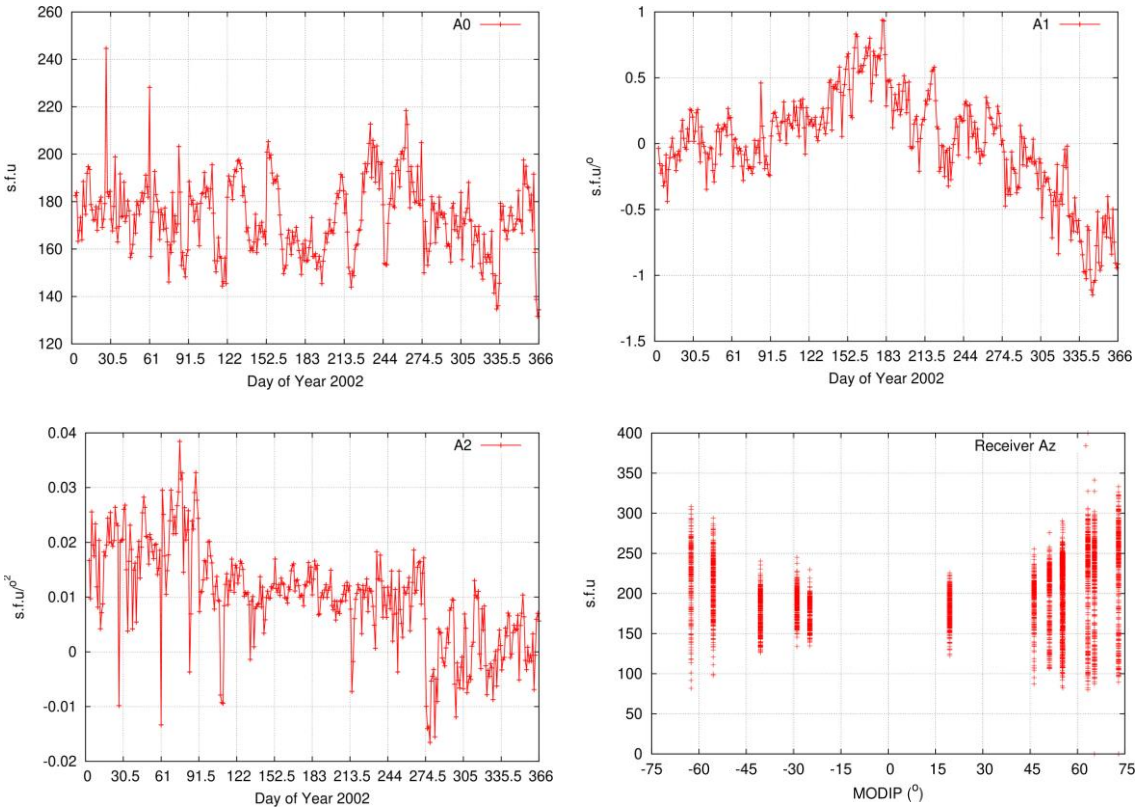

Figure 13. Az parameters computed with IGS receivers for 2002, along with the individual Az values for the whole year (right-bottom panel).

The same methodology to compute the positioning error and the same network of IGS stations used to derive the results in Section 6.2.2 has been replicated here.

The following plots show the global mean of the 68th, 90th and 95th percentiles of the 3D position error computed on a daily basis at each individual station for the year 2002. These results show that for the simulated case both models present a very similar performance in the PVT algorithm.

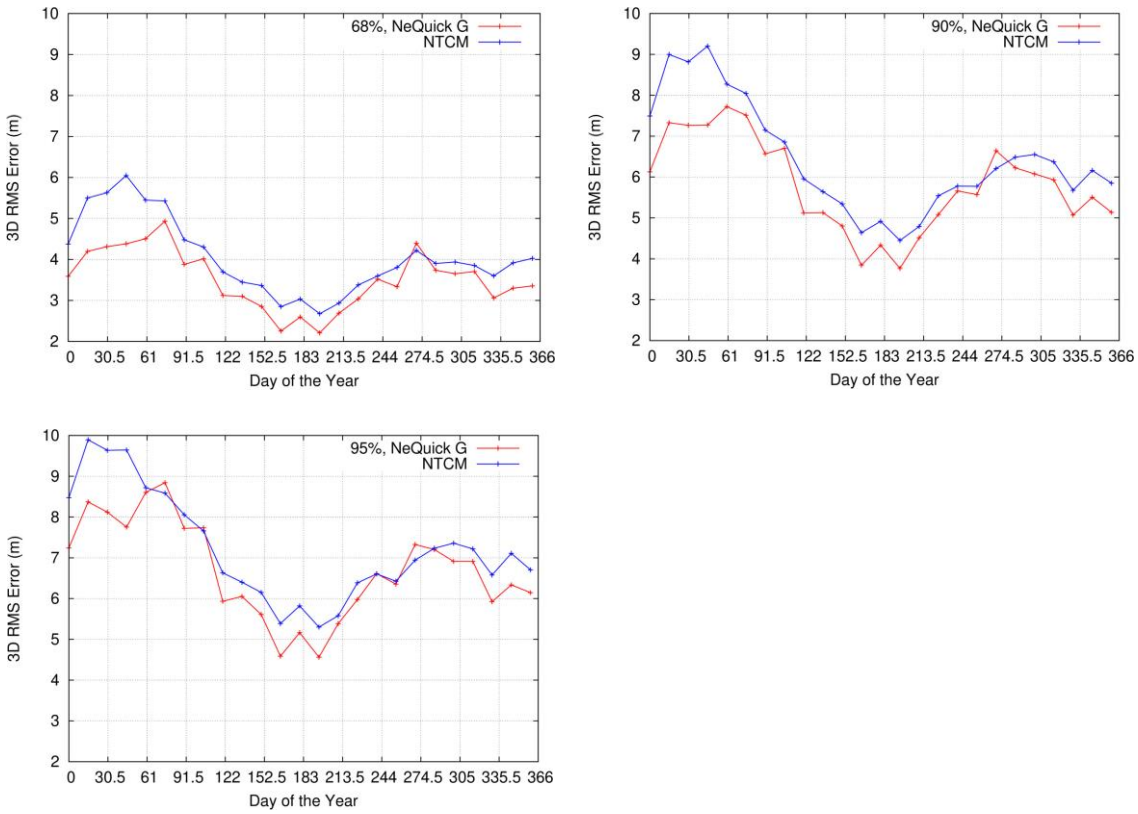

Figure 14. 3D error as a function of the day for different percentiles and models for 2002. Notice that the points corresponds to the weighted 15-day average.

7. Annex D – *Input/Output Verification Data*

The test vectors provided in this appendix are valid for the current Galileo Single Frequency Ionospheric Model *NTCM G* v1.0 available at the website of the European GNSS Service Centre (GSC) https://www.gsc-europa.eu/. They provide the input and the expected output in order to verify the correctness of a particular software implementation of *NTCM G*.

7.1 Az coefficients (high solar activity)

a_0	a_1	a_2
236.831641	-0.39362878	0.00402826613

Input								Output
Day of Year	Time (UT)	Station Longitude (deg)	Station Latitude (deg)	Station Height (m)	Satellite Longitude (deg)	Satellite Latitude (deg)	Satellite Height (m)	STEC (TECU)
105	0	-62.34	82.49	78.11	8.23	54.29	20281546.18	33.7567
105	0	-62.34	82.49	78.11	-158.03	24.05	20275295.43	98.7476
105	0	-62.34	82.49	78.11	-30.86	41.04	19953770.93	42.2768
105	4	-62.34	82.49	78.11	-85.72	53.69	20544786.65	32.1058
105	4	-62.34	82.49	78.11	-130.77	54.40	20121312.46	33.6307
105	4	-62.34	82.49	78.11	140.68	35.85	19953735.00	54.6962
105	8	-62.34	82.49	78.11	-126.28	51.26	20513440.10	30.8902
105	8	-62.34	82.49	78.11	84.26	54.68	20305726.79	33.8241
105	8	-62.34	82.49	78.11	-96.21	37.33	19956072.48	36.9695
105	12	-62.34	82.49	78.11	81.09	35.20	20278071.03	65.0500
105	12	-62.34	82.49	78.11	175.57	51.89	19995445.72	33.9561
105	12	-62.34	82.49	78.11	4.25	53.43	20107681.66	40.4107
105	16	-62.34	82.49	78.11	14.89	32.88	20636367.33	73.7953
105	16	-62.34	82.49	78.11	-70.26	50.63	20043030.82	47.1845
105	16	-62.34	82.49	78.11	-130.60	49.21	20288021.34	46.4704
105	20	-62.34	82.49	78.11	-52.46	24.28	19831557.96	87.9216
105	20	-62.34	82.49	78.11	-165.78	35.06	20196268.24	69.7195
105	20	-62.34	82.49	78.11	168.73	52.58	20288372.95	44.4995
105	0	-52.81	5.25	-25.76	-89.48	-29.05	20081457.33	125.2377
105	0	-52.81	5.25	-25.76	-46.73	-24.08	19975517.42	86.3239
105	0	-52.81	5.25	-25.76	-99.26	34.47	20275286.46	127.0015
105	4	-52.81	5.25	-25.76	-46.61	54.84	20258938.89	75.5439
105	4	-52.81	5.25	-25.76	-85.72	53.68	20544786.61	86.2081
105	4	-52.81	5.25	-25.76	-18.13	14.17	20267783.18	59.7016
105	8	-52.81	5.25	-25.76	7.14	-19.55	20226657.45	83.0316
105	8	-52.81	5.25	-25.76	-48.38	-31.04	20069586.93	39.9556
105	8	-52.81	5.25	-25.76	-58.59	21.93	20008556.82	31.4675
105	12	-52.81	5.25	-25.76	-102.83	-40.74	20153844.84	194.4159
105	12	-52.81	5.25	-25.76	-0.60	10.75	20272829.17	181.2492
105	12	-52.81	5.25	-25.76	-120.35	11.00	20283503.35	184.0749
105	16	-52.81	5.25	-25.76	-70.26	50.63	20043030.72	216.2278
105	16	-52.81	5.25	-25.76	-72.73	-9.78	19936049.27	162.4852
105	16	-52.81	5.25	-25.76	-66.77	2.37	19986966.89	147.7473
105	20	-52.81	5.25	-25.76	-1.57	-7.90	20373709.74	220.0012
105	20	-52.81	5.25	-25.76	0.44	50.83	19975412.45	240.8009
105	20	-52.81	5.25	-25.76	10.94	44.72	20450566.19	252.0204

7.2 Az coefficients (medium solar activity)

a_0	a_1	a_2
121.129893	0.351254133	0.0134635348

Input								Output
Day of Year	Time (UT)	Station Longitude (deg)	Station Latitude (deg)	Station Height (m)	Satellite Longitude (deg)	Satellite Latitude (deg)	Satellite Height (m)	STEC (TECU)
105	0	40.19	-3.00	-23.32	76.65	-41.43	20157673.93	28.3208
105	0	40.19	-3.00	-23.32	-13.11	-4.67	20194168.22	36.9892
105	0	40.19	-3.00	-23.32	26.31	-39.04	20671871.64	24.3477
105	4	40.19	-3.00	-23.32	79.33	-55.34	20679595.44	72.4723
105	4	40.19	-3.00	-23.32	107.19	-10.65	19943686.06	108.8940
105	4	40.19	-3.00	-23.32	56.35	47.54	20322471.38	66.2816
105	8	40.19	-3.00	-23.32	7.14	-19.55	20226657.34	98.5299
105	8	40.19	-3.00	-23.32	51.96	-1.90	20218595.37	78.9012
105	8	40.19	-3.00	-23.32	89.22	-40.56	20055109.63	149.9891
105	12	40.19	-3.00	-23.32	90.78	-28.26	20081398.25	153.7801
105	12	40.19	-3.00	-23.32	35.75	-14.88	20010521.91	88.5214
105	12	40.19	-3.00	-23.32	81.09	35.20	20278071.09	161.6302
105	16	40.19	-3.00	-23.32	14.89	32.88	20636367.52	86.2076
105	16	40.19	-3.00	-23.32	2.04	11.23	20394926.95	83.4856
105	16	40.19	-3.00	-23.32	22.79	-35.87	20125991.19	73.8076
105	20	40.19	-3.00	-23.32	54.11	3.15	20251696.28	36.3307
105	20	40.19	-3.00	-23.32	95.06	17.94	20246498.07	69.0422
105	20	40.19	-3.00	-23.32	-1.81	-52.00	20332764.38	69.9599
105	0	115.89	-31.80	12.78	119.90	-8.76	19941513.27	23.8358
105	0	115.89	-31.80	12.78	165.14	-13.93	20181976.57	38.5473
105	0	115.89	-31.80	12.78	76.65	-41.43	20157673.77	23.6849
105	4	115.89	-31.80	12.78	107.19	-10.65	19943685.24	40.8648
105	4	115.89	-31.80	12.78	79.33	-55.34	20679595.29	44.0008
105	4	115.89	-31.80	12.78	64.90	-17.58	20177185.06	57.6945
105	8	115.89	-31.80	12.78	127.35	23.46	19837695.71	82.6376
105	8	115.89	-31.80	12.78	89.22	-40.56	20055109.56	39.1752
105	8	115.89	-31.80	12.78	148.31	-29.93	20109263.99	40.6714
105	12	115.89	-31.80	12.78	90.78	-28.26	20081398.25	23.2595
105	12	115.89	-31.80	12.78	133.47	-24.87	19975574.41	21.5454
105	12	115.89	-31.80	12.78	166.97	-3.87	20196778.56	38.6379
105	16	115.89	-31.80	12.78	124.09	-14.31	20100697.90	15.0902
105	16	115.89	-31.80	12.78	154.31	-45.19	20116286.17	16.5133
105	16	115.89	-31.80	12.78	-167.50	-43.24	20095343.13	25.6441
105	20	115.89	-31.80	12.78	131.65	-31.56	20066111.12	7.5508
105	20	115.89	-31.80	12.78	115.68	-52.78	20231909.06	7.8470
105	20	115.89	-31.80	12.78	50.87	-50.69	20186511.77	12.4908

7.3 Az coefficients (low solar activity)

a_0	a_1	a_2
2.580271	0.127628236	0.0252748384

Input								Output
Day of Year	Time (UT)	Station Longitude (deg)	Station Latitude (deg)	Station Height (m)	Satellite Longitude (deg)	Satellite Latitude (deg)	Satellite Height (m)	STEC (TECU)
105	0	141.13	39.14	117.00	165.14	-13.93	20181976.50	51.5270
105	0	141.13	39.14	117.00	85.59	36.64	20015444.79	25.3869
105	0	141.13	39.14	117.00	119.90	-8.76	19941513.27	40.6363
105	4	141.13	39.14	117.00	107.19	-10.65	19943685.88	67.1614
105	4	141.13	39.14	117.00	38.39	51.98	20457198.52	41.9432
105	4	141.13	39.14	117.00	-130.77	54.40	20121312.41	38.0286
105	8	141.13	39.14	117.00	179.50	51.35	19967933.94	20.6012
105	8	141.13	39.14	117.00	97.28	21.46	19941941.52	30.6540
105	8	141.13	39.14	117.00	84.26	54.68	20305726.98	25.3269
105	12	141.13	39.14	117.00	62.65	54.77	20370905.24	18.7723
105	12	141.13	39.14	117.00	115.63	-1.28	20165065.92	22.6981
105	12	141.13	39.14	117.00	81.09	35.20	20278071.22	19.0137
105	16	141.13	39.14	117.00	124.09	-14.31	20100698.19	20.1095
105	16	141.13	39.14	117.00	-130.60	49.21	20288020.98	12.3098
105	16	141.13	39.14	117.00	161.97	13.35	20265041.53	10.1019
105	20	141.13	39.14	117.00	84.18	36.59	19953853.27	10.2320
105	20	141.13	39.14	117.00	54.67	51.65	20511861.27	11.6913
105	20	141.13	39.14	117.00	-136.92	46.53	20309713.36	15.2671
105	0	-155.46	19.80	3754.69	165.14	-13.93	20181976.58	67.7247
105	0	-155.46	19.80	3754.69	179.32	9.92	20274303.54	41.9874
105	0	-155.46	19.80	3754.69	-144.16	-15.44	20007317.84	50.6599
105	4	-155.46	19.80	3754.69	-130.77	54.40	20121312.45	32.8732
105	4	-155.46	19.80	3754.69	-99.26	37.44	20066769.88	39.5971
105	4	-155.46	19.80	3754.69	-85.72	53.69	20544786.60	41.9149
105	8	-155.46	19.80	3754.69	178.35	-7.05	20372509.81	22.7673
105	8	-155.46	19.80	3754.69	-125.97	2.30	20251559.90	20.2296
105	8	-155.46	19.80	3754.69	179.50	51.35	19967934.29	19.9825
105	12	-155.46	19.80	3754.69	158.88	-12.61	20145417.20	22.1744
105	12	-155.46	19.80	3754.69	-146.53	22.03	20069033.97	9.7271
105	12	-155.46	19.80	3754.69	-153.30	-39.75	20672066.87	21.9415
105	16	-155.46	19.80	3754.69	-140.58	51.70	20455387.61	12.7349
105	16	-155.46	19.80	3754.69	-167.50	-43.24	20095343.11	25.0219
105	16	-155.46	19.80	3754.69	-164.50	27.08	20494802.61	10.4564
105	20	-155.46	19.80	3754.69	-172.71	-20.37	20225145.06	44.0358
105	20	-155.46	19.80	3754.69	-136.92	46.53	20309713.37	31.7940
105	20	-155.46	19.80	3754.69	-82.52	20.64	19937791.48	67.4750


EUROPEAN GNSS (GALILEO)
OPEN SERVICE
PROGRAMME OF THE
EUROPEAN UNION
GALILEO
EGNOS